Parameterizing Quasi-Periodicity: Generalized Poisson Summation and Its Application to Modified-Fibonacci Antenna Arrays

Vincenzo Galdi, *Senior Member, IEEE*, Giuseppe Castaldi, Vincenzo Pierro, Innocenzo M. Pinto, *Member, IEEE*, and Leopold B. Felsen, *Life Fellow, IEEE*

***Abstract*—The fairly recent discovery of "quasi-crystals," whose X-ray diffraction patterns reveal certain peculiar features which do not conform with spatial periodicity, has motivated studies of the wave-dynamical implications of "aperiodic order." Within the context of the radiation properties of antenna arrays, an instructive novel (canonical) example of wave interactions with *quasi-periodic* order is illustrated here for one-dimensional array configurations based on the "modified-Fibonacci" sequence, with utilization of a two-scale generalization of the standard Poisson summation formula for periodic arrays. This allows for a "quasi-Floquet" analytic parameterization of the radiated field, which provides instructive insights into some of the basic wave mechanisms associated with quasi-periodic order, highlighting similarities and differences with the periodic case. Examples are shown for quasi-periodic infinite and spatially-truncated arrays, with brief discussion of computational issues and potential applications.**

***Index Terms*—Antenna arrays, aperiodic order, Fibonacci sequence, generalized Poisson summation.**

I. Introduction

THE recent discovery (1984) of "quasi-crystals," i.e., certain metallic alloys whose X-ray diffraction patterns contain bright spots displaying symmetries (e.g., 5-fold) which are *incompatible* with *spatial periodicity* [1], [2], has stimulated a growing interest in the study of *aperiodic order* and its wave-dynamical properties.

In electromagnetics (EM) engineering, use of random or deterministic *aperiodic* geometries has been customary within the framework of antenna array *thinning* [3]–[5], whereas *multiperiod* configurations have recently been proposed for optimizing the passband/stopband characteristics of frequency selective surfaces [6] and photonic bandgap (PBG) devices [7]. In [8], we explored the radiation properties of two-dimensional (2-D) antenna arrays based on the concept of "aperiodic tiling" [9], [10], which had previously found interesting applications in the field of PBG devices (see the brief summary and references in [8]).

Manuscript received October 12, 2004. The work of L. B. Felsen was supported in part by Polytechnic University, Brooklyn, NY, 11201, USA.

V. Galdi, G. Castaldi, V. Pierro and I. M. Pinto are with the Waves Group, Department of Engineering, University of Sannio, I-82100 Benevento, Italy (e-mail: vgaldi@unisannio.it, castaldi@unisannio.it, pierro@unisannio.it, pinto@sa.infn.it).

L. B. Felsen is with the Department of Aerospace and Mechanical Engineering and Department of Electrical and Computer Engineering, Boston University, Boston, MA 02215 USA and also with Polytechnic University, Brooklyn, NY 11201 USA (e-mail: lfelsen@bu.edu).

Digital Object Identifier 10.1109/TAP.2005.848514

In this paper, we turn our attention to the radiation properties of a different category of aperiodic structures consisting of two-scale Fibonacci-type sequences [11]. Materials exhibiting this type of aperiodic order, technically called "quasi-periodicity" (see the definition in Section II-B), were first fabricated in 1985 as GaAs-AlAs heterostructures (1-D multilayers) [12]; their technical classification as "quasi-crystals" is still debated [13]. The wave-dynamical properties of 1-D and 2-D Fibonacci-type structures have been widely investigated, theoretically and experimentally, in quantum mechanics, acoustics and EM (see [14]–[26] for a sparse sampling). Particularly interesting outcomes concern the self-similar fractal (Cantor-type) nature of the eigenspectra [14], [16], [20], and the possible presence of bandgaps [19], [21], omnidirectional reflection properties [22], [25], and localization phenomena [14], [18], [23].

Here, we concentrate on the study of the radiation properties of a simple class of 1-D antenna arrays based on the so-called "modified-Fibonacci" sequence. This novel prototype array configuration appears particularly well suited to exploration of some basic characteristics of wave interactions with quasi-periodic order. First, this array model is amenable to *analytic* parameterization via a *generalized Poisson summation* formula, by exploiting some recent results in [27] (this paper is easily accessible through the web). Note that, in principle, one can derive generalized Poisson summation formulas that accommodate a variety of "nonperiodicity scales" (see, e.g., [28]). Here, we consider only two scales, d_1 and d_2. This opens up the possibility of extending the Floquet-based parameterization of infinite and semi-infinite time-harmonic *periodic* arrays in [29], [30] to the case of two-scale *quasi-periodic* arrays. Next, the inherent degree of freedom in the choice of the ratio between the two scales can be used to study the "transition" from periodic ($d_1 = d_2$) to quasi-periodic ($d_1 \neq d_2$) order, so as to better understand the quasi-periodicity-induced footprints in the wave dynamics. Finally, although the main focus of this preliminary investigation is on wave-dynamical phenomenologies, computational and applicational issues for a test example are briefly addressed as well, including possible exploitation of the two-scale degree of freedom for pattern control in practical applications.

The paper is organized as follows. In Section II, the problem geometry is described, and the modified-Fibonacci sequence is introduced together with general aspects of quasi-periodicity. In Section III, the generalized Poisson summation formula for modified-Fibonacci arrays is introduced, and its similarities and

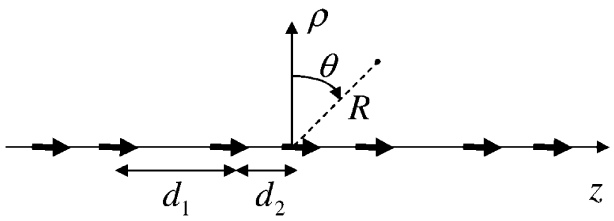

Fig. 1. Problem schematic: An infinite (or semi-infinite) phased line array of z-directed electric dipoles is considered. The dipole distribution z_m, which features only two possible interelement spacings d_1 and $d_2 \leq d_1$, is chosen according to the modified-fibonacci sequence in (5). Also shown are the (z, ρ) and (R, θ) coordinate systems utilized.

differences with the periodic case are discussed. In Section IV, a "quasi-Floquet" (QF) parameterization of the radiated field for infinite and semi-infinite modified-Fibonacci arrays is derived, paralleling [29], [30]. Numerical results and potential applications are illustrated in Section V, followed by brief concluding remarks in Section VI.

II. Background and Problem Formulation

A. Geometry

Referring to the geometry depicted in Fig. 1, we begin with an infinite phased line array of z-directed electric dipoles, subject to uniform unit-amplitude time-harmonic $\exp(j\omega t)$ excitation, described by the current distribution

$$f(z) = \sum_{m=-\infty}^{\infty} \delta(z - z_m) \exp(-j\eta k_0 z_m) \tag{1}$$

where $k_0 = \omega\sqrt{\epsilon_0 \mu_0} = 2\pi/\lambda_0$ is the free-space wavenumber (with λ_0 being the wavelength), and $-1 \leq \eta \leq 1$ describes the interelement phasing. The dipole sequence $\{z_m\}_{m=-\infty}^{\infty}$, which is restricted to two possible interelement spacings d_1 and $d_2 \leq d_1$ (see Fig. 1), is chosen according to the modified-Fibonacci rule, whose properties are summarized below. Spatial truncation effects will be discussed in Section IV-B.

B. Modified-Fibonacci Sequence: An Example of Quasi-Periodic Order

The Fibonacci sequence [11], introduced in 1202 by the Italian mathematician Leonardo da Pisa (Fibonacci) (ca. 1170–ca. 1240), in connection with a model for rabbit breeding, is probably the earliest and most thoroughly investigated deterministic aperiodic sequence. Since then, it has found applications in many different fields, owing to its intimate relation with one of the most pervasive mathematical entities, the *Golden Mean* [11]. In its simplest version, the Fibonacci sequence can be generated from a two-symbol alphabet $\mathcal{A} = \{a, b\}$, by iteratively applying the substitution rules

$$a \to ab, \quad b \to a \tag{2}$$

so as to construct a sequence of symbolic strings s_n

$$b \Rightarrow a \Rightarrow ab \Rightarrow aba \Rightarrow abaab \Rightarrow abaababaab \Rightarrow abaababaabaab \cdots. \tag{3}$$

Note that the string at each iteration is obtained as the concatenation of the two preceding ones ($s_n = s_{n-1} \cup s_{n-2}$). The process can be iterated *ad infinitum*, yielding an infinite sequence of "a" and "b" symbols which seems to display no apparent regularity, but actually hides a wealth of interesting properties (see [11] for details). For instance, in the limit of an infinite sequence, it can be shown that the ratio between the numbers of "a" and "b" symbols (N_a and N_b, respectively) approaches the Golden Mean $\tau = (1 + \sqrt{5})/2$[11]

$$\lim_{N \to \infty} \frac{N_a}{N_b} = \tau = \frac{1 + \sqrt{5}}{2}, \quad N_a + N_b = N. \tag{4}$$

In connection with the antenna array problem of interest here, there are several ways of embedding the above-introduced Fibonacci-type aperiodic sequence. One possibility would be keeping the geometry *periodic* (i.e., uniform interelement spacing) and associating with the "a" and "b" symbols in the Fibonacci sequence two possible current amplitudes. Another possibility, pursued in this investigation, assumes *uniform excitation* and associates the "a" and "b" symbols with two possible interelement spacings, d_1 and $d_2 \leq d_1$, respectively (see Fig. 1). Accordingly, the dipole positions z_m in (1) can be obtained from the symbolic strings in (3) or, in an equivalent and more direct fashion, via [27]

$$z_m = d_1 \left\| \frac{m}{\tau} \right\| + d_2 \left(m - \left\| \frac{m}{\tau} \right\| \right) \tag{5}$$

where $\|\cdot\|$ denotes the nearest-integer function,

$$\|x\| = \begin{cases} m, & m \leq x < m + \frac{1}{2} \\ m + 1, & m + \frac{1}{2} \leq x \leq m + 1. \end{cases} \tag{6}$$

Following [27], the particular case $d_2 = d_1/\tau$ in (5) will be referred to as "standard Fibonacci." The general case, in which the scale ratio $\nu = d_2/d_1$ is left as a degree of freedom, will be referred to as "modified Fibonacci", and represents one of the simplest extensions of the Fibonacci sequence. The reader is referred to [28], [31], [32] for other examples of possible extensions/generalizations.

Note that the modified-Fibonacci sequence in (5) includes as a limit the *periodic* case ($d_1 = d_2$). It can be proved that, with the exception of this degenerate case, the sequence in (5) and the corresponding dipole distribution in (1) display a "quasi-periodic" character, which represents one of the most common and best known forms of aperiodic order. The concept of quasi-periodicity stems from the theory of "almost-periodic" functions developed by H. Bohr during the 1920s [33], [34]. In essence, a quasi-periodic function can be uniformly approximated by a generalized Fourier series containing a countable infinity of *pairwise incommensurate* frequencies generated from a finite-dimensional basis (see [33], [34] for more details).

It follows from (4) that, in the infinite-sequence limit, the average interelement spacing d_{av} is [27]

$$d_{av} = \frac{\tau d_1 + d_2}{1 + \tau}. \tag{7}$$

Anticipating the analytic derivations and parametric analysis in Sections III and IV, it is expedient to parameterize the sequence

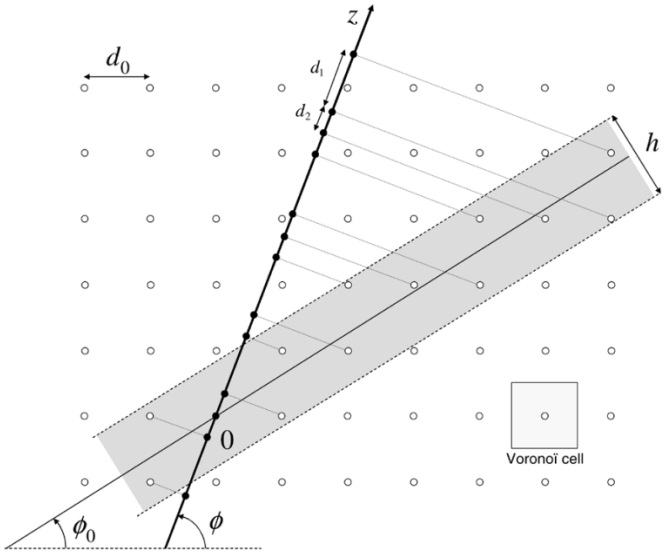

Fig. 2. "Cut-and-project" graphic interpretation of the modified-Fibonacci sequence in (5). A 2-D square lattice of side $d_0 = d_1\sqrt{1+\nu^2}$ is traversed by a straight line with slope $\tan\phi_0 = 1/\tau$, and those lattice points whose "Voronoï cell" (light-shaded square cell of side d_0 centered around the point) is crossed by the line (or, equivalently, those falling within the dark-shaded rectangular window of size $h = d_0(1+\tau)/\sqrt{2+\tau}$ centered around the line) are orthogonally projected onto another straight line (z-axis) with slope $\tan\phi = \nu$. For the standard-Fibonacci sequence ($\nu = 1/\tau$), the two lines coincide ($\phi = \phi_0$).

in (5) in terms of the average spacing d_{av} in (7) and the scale ratio $\nu = d_2/d_1$, rewriting d_1 and d_2 as

$$d_1 = \frac{(1+\tau)}{(\nu+\tau)}d_{av}, \quad d_2 = \nu d_1, \;\; 0 < \nu \leq 1. \tag{8}$$

The modified-Fibonacci sequence in (5) admits an instructive alternative interpretation in terms of a "cut-and-project" graphic construction [27], as illustrated in Fig. 2. Cut-and-project schemes are systematic tools for generating *quasi-periodic* sets via projection from higher-dimensional *periodic* lattices (see [10] for details). In our case, one starts from a 2-D square lattice of side $d_0 = d_1\sqrt{1+\nu^2}$ traversed by a straight line with slope $\tan\phi_0 = 1/\tau$. Those lattice points whose "Voronoï cell" [10] (light-shaded square cell of side d_0 centered around the point, in Fig. 2) is crossed by the line (or, equivalently, those falling within the rectangular window of size $h = d_0(1+\tau)/\sqrt{2+\tau}$ centered around the line, in Fig. 2) are orthogonally projected onto another straight line (z-axis in Fig. 2) with slope $\tan\phi = \nu$ to yield the desired modified-Fibonacci sequence in (5). For the standard-Fibonacci sequence ($\nu = 1/\tau$), the two lines coincide ($\phi = \phi_0$) and the above scheme becomes equivalent to the canonical cut-and-project scheme described in [10].

III. Generalized Poisson Summation Formula

For *periodic* structures, Floquet theory provides a rigorous and powerful framework for spectral- or spatial-domain analytic and numerical analysis. In this connection, the Poisson summation formula [35] can be utilized to systematically recast field observables as superpositions of either *individual* or *collective* contributions. Problem-matched extensions have also been developed to accommodate typical departures from perfect periodicity in realistic structures, such as truncation (finiteness) and *smooth* perturbations in the spatial period as well as in the excitation (tapering) [36]–[39].

Considering the degenerate *periodic* limiting case ($d_1 = d_2 = d$, i.e., $z_m = md$) of the modified-Fibonacci sequence in (5) , the corresponding periodic limit $f^{(\mathrm{per})}$ of the current distribution in (1) can be recast, via the standard Poisson summation formula [35], as

$$f^{(\mathrm{per})}(z) = \sum_{m=-\infty}^{\infty} \delta(z-md)\exp(-j\eta k_0 md) \tag{9a}$$

$$= \frac{1}{d}\sum_{q=-\infty}^{\infty} \exp(-jk_{zq}z)$$

$$k_{zq} = k_0\eta + \frac{2\pi q}{d}. \tag{9b}$$

The m-indexed *individual* dipole contributions in (9a) are thereby recast into the infinite superposition of linearly smoothly-phased q-indexed equivalent line source distributions in (9b). Remarkably, a similar re-parameterization is *always* possible for the *general* (i.e., *quasi-periodic*) case of the modified-Fibonacci sequence in (5), since it can be shown that the spatial Fourier transform (plane-wave spectrum) of (1) can be written as [27] (see also Appendix)

$$\hat{F}(k_z) = \int_{-\infty}^{\infty} f(z)\exp(jk_z z)dz$$

$$= \sum_{m=-\infty}^{\infty} \exp(jk_z z_m)\exp(-j\eta k_0 z_m) \tag{10a}$$

$$= \frac{2\pi}{d_{av}}\sum_{q_1,q_2=-\infty}^{\infty} S_{q_1q_2}\delta(k_z - k_{zq_1q_2}) \tag{10b}$$

where d_{av} is defined in (7), and the amplitude coefficients $S_{q_1q_2}$ and the spatial frequencies $k_{zq_1q_2}$ are given by

$$S_{q_1q_2} = \frac{\sin W_{q_1q_2}}{W_{q_1q_2}}$$

$$W_{q_1q_2} = \frac{\pi}{d_{av}}(q_1d_1 - q_2d_2) = \frac{\pi(1+\tau)(q_1-q_2\nu)}{\nu+\tau} \tag{11}$$

$$k_{zq_1q_2} = k_0\eta + \alpha_{q_1q_2}, \quad \alpha_{q_1q_2} = \frac{2\pi}{d_{av}}\frac{(q_1+q_2\tau)}{(\tau+1)}. \tag{12}$$

It then follows via straightforward inverse Fourier transform of (10b) that

$$f(z) = \frac{1}{d_{av}}\sum_{q_1,q_2=-\infty}^{\infty} S_{q_1q_2}\exp(-jk_{zq_1q_2}z). \tag{13}$$

Equation (13) thus represents a generalization of the standard Poisson summation formula for *periodic* arrays in (9) to the more general *quasi-periodic* modified-Fibonacci array in (5), and will accordingly be referred to as *generalized* Poisson summation formula. It is readily verified that for the special case of *periodic* arrays ($d_1 = d_2 = d$, i.e., $\nu = 1$), one obtains

$$d_{av} = d, \quad W_{q_1q_2} = (q_1-q_2)\pi, \quad S_{q_1q_2} = \delta_{q_1q_2} \tag{14}$$

with $\delta_{q_1 q_2}$ denoting the Kronecker delta, and thus (13) reduces to the standard Poisson summation formula in (9b).

A few observations are in order to highlight similarities and differences between (13) and (9). Similar to (9), the *individual* dipole contributions in (5) are recast via (13) as a superposition of *collective* contributions arising from linearly smoothly-phased equivalent line source distributions. However, at variance with the q-indexed *single* infinity of *equispaced* spatial frequencies in (9b), the generalized Poisson summation formula in (13) entails a (q_1, q_2)-indexed *double* infinity of generally *pairwise-incommensurate* spatial frequencies. This could be expected recalling the definition of the quasi-periodic functions given in Section II-B. Note that the spatial frequencies $k_{zq_1q_2}$ in (12) depend on the average interelement spacing d_{av}, but are *independent* of the scale ratio $\nu = d_2/d_1$. The dependence on ν shows up (via $W_{q_1q_2}$) in the amplitude coefficients $S_{q_1q_2}$ in (11), which are not constant as for the periodic case in (9b). It is worth pointing out that such dependence is *smooth*, and consequently no *abrupt* transition occurs when ν is varied between *rational* and *irrational* values, i.e., going from *commensurate* to *incommensurate* scales d_1 and d_2. However, for the case of *commensurate* scales

$$\nu = \frac{d_2}{d_1} = \frac{p_1}{p_2}, \quad p_1, p_2 \in \mathbb{N} \tag{15}$$

one can readily verify that

$$\begin{aligned} k_{z(q_1+Mp_1)(q_2+Mp_2)} &= k_{zq_1q_2} + M\left(\frac{2\pi}{d_1}p_2\right) \\ W_{(q_1+Mp_1)(q_2+Mp_2)} &= W_{q_1q_2}, \quad M \in \mathbb{Z} \end{aligned} \tag{16}$$

and thus the array spectrum in (10b) is *periodic* with period $2\pi p_2/d_1$. It can be verified that the opposite implication is also true, and thus the spectrum is periodic *if and only if* the scales d_1 and d_2 are commensurate, although the array remains *aperiodic* in physical space [27].

IV. Radiated Field

In order to further explore possible similarities and differences between the wave phenomenologies associated with *periodicity* and *quasi-periodicity*, it is instructive to consider the radiated fields. To this end, in what follows, we extend the Floquet-based frequency-domain analysis in [29], [30], for infinite and semi-infinite periodic phased arrays of dipoles, to the quasi-periodic modified-Fibonacci case. As in [29], [30], attention is restricted to the z-directed vector potential $\mathbf{A}(\mathbf{r}) = A(\mathbf{r})\mathbf{u}_z$, with $\mathbf{r} \equiv (z, \rho)$ and with $\mathbf{u}_z$ denoting a z-directed unit vector, from which all field quantities of interest can be computed. Whenever applicable, partial results from [29], [30] are recalled and used, without going into the details of the technical derivations.

A. Infinite Arrays

For infinite arrays, proceding analogous to [29], the generalized Poisson summation formula in (13) can be used to recast the element-by-element (spherical wave) synthesis of the field potential

$$\begin{aligned} A(\mathbf{r}) &= \int_{-\infty}^{\infty} f(z') \frac{\exp(-jk_0R)}{4\pi R} dz' = \sum_{m=-\infty}^{\infty} A_m(\mathbf{r}) \\ &= \sum_{m=-\infty}^{\infty} \frac{\exp(-jk_0R_m)}{4\pi R_m} \exp(-jk_0\eta z_m) \end{aligned} \tag{17}$$

where $R = \sqrt{\rho^2 + (z-z')^2}$ and $R_m = \sqrt{\rho^2 + (z-z_m)^2}$, in terms of a "quasi-Floquet" (QF) representation

$$A(\mathbf{r}) = \sum_{q_1, q_2 = -\infty}^{\infty} S_{q_1q_2} A^{\mathrm{QF}}_{q_1q_2}(\mathbf{r}) \tag{18}$$

$$\begin{aligned} A^{\mathrm{QF}}_{q_1q_2}(\mathbf{r}) &= \frac{1}{d_{av}} \int_{-\infty}^{\infty} \frac{\exp(-jk_0R)}{4\pi R} \exp(-jk_{zq_1q_2}z')\, dz' \\ &= \frac{\exp(-jk_{zq_1q_2}z)}{4jd_{av}} \mathrm{H}_0^{(2)}(k_{\rho q_1q_2}\rho). \end{aligned} \tag{19}$$

In (19), $\mathrm{H}_0^{(2)}$ denotes the zeroth-order Hankel function of the second kind (line-source Green's function), and $k_{\rho q_1 q_2} = \sqrt{k_0^2 - k_{zq_1q_2}^2}$, $\mathrm{Im}(k_{\rho q_1 q_2}) \leq 0$ denote the QF wave radial wavenumbers related to the z-domain wavenumbers $k_{zq_1q_2}$ in (12). Recalling the asymptotic ($|k_{\rho q_1 q_2}\rho| \to \infty$) expansion of the Hankel function, one obtains

$$\begin{aligned} A^{\mathrm{QF}}_{q_1q_2}(\mathbf{r}) \sim{}& \frac{1}{d_{av}\sqrt{4\pi k_{\rho q_1q_2}\rho}} \\ &\times \exp\left[-j\left(k_{\rho q_1q_2}\rho + k_{zq_1q_2}z + \frac{\pi}{4}\right)\right] \end{aligned} \tag{20}$$

from which it is recognized that

$$|k_{zq_1q_2}| < k_0, \quad q_2 \lessgtr -\frac{q_1}{\tau} \pm \left(\frac{d_{av}}{\lambda_0}\right)\frac{(1 \mp \eta)(1+\tau)}{\tau} \tag{21}$$

corresponds to *radially-propagating* QF waves, whereas $|k_{zq_1q_2}| > k_0$ corresponds to *radially-evanescent* QF waves. Accordingly, sufficiently far from the array axis, the potential

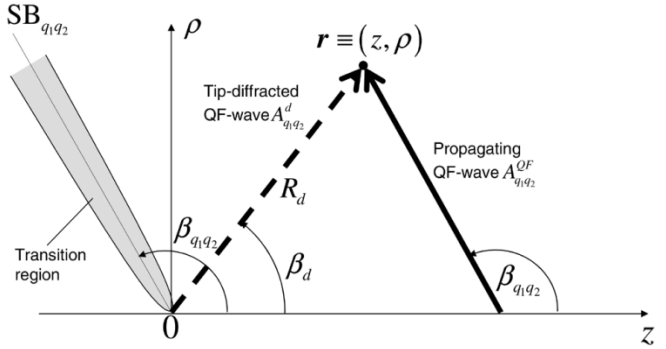

Fig. 3. Quasi-Floquet (QF) wave phenomenologies for the infinite and semi-infinite array (planar cut through conical wavefields). For the infinite array, the wavefield away from the array axis is synthesized in terms of propagating QF waves $A^{\mathrm{QF}}_{q_1q_2}$ (heavy solid arrow) arriving from direction $\beta_{q_1q_2}$ in (22). For the semi-infinite array, the region of validity of each propagating QF wave is limited by a conical shadow boundary $\mathrm{SB}_{q_1q_2}$ with the same angle $\beta_{q_1q_2}$. A spherical tip-diffracted QF wave $A^d_{q_1q_2}$ (dashed arrow) arriving from direction β_d ensures, via the transition function in (27), continuity of the wavefield across the parabolic transition region (gray shading) surrounding the shadow boundary cone.

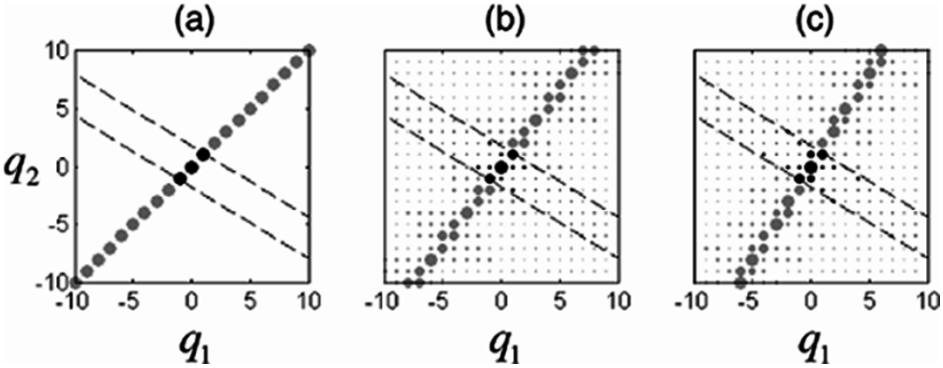

Fig. 4. Modified-Fibonacci array with $d_{av} = 1.1\lambda_0, \eta = 0$, and various values of the scale ratio $\nu = d_2/d_1$. (q_1, q_2)-plane mapping of propagating (dark dots) and evanescent (light dots) amplitude coefficients $S_{q_1 q_2}$ in (11). Only $|q_1|, |q_2| \leq 10$ spatial frequencies are considered, with dot size proportional to coefficient amplitude. The two oblique dashed lines delimit the propagating spectral range in (21). (a): $\nu = 1$ (periodic); (b): $\nu = 0.75$; (c): $\nu = 1/\tau$ (standard-Fibonacci).

field in (18) will be synthesized in terms of *conical* propagating QF waves (heavy solid arrow in Fig. 3), with arrival directions

$$\beta_{q_1 q_2} = \arccos\left(\frac{k_{z q_1 q_2}}{k_0}\right). \tag{22}$$

In the (q_1, q_2)-plane, the propagating spectral range in (21) is mapped into an *infinite* strip, thus indicating the general presence of an *infinite* number of propagating QF waves. This is illustrated in Fig. 4, for a nonphased $(\eta = 0)$ array with $d_{av} = 1.1\lambda_0$ and various values of the scale ratio $\nu = d_2/d_1$. Also shown, for comparison, is the *periodic* case [Fig. 4(a)], which entails a *finite* number of propagating Floquet waves. In the general *quasi-periodic* case, it is observed that the propagating spectral range is vastly populated, irrespective of the commensurate [Fig. 4(b)] or incommensurate [Fig. 4(c)] character of the scales d_1 and d_2. However, it follows from (11) that moving toward large values of q_1, q_2 (with opposite sign), the amplitude coefficients $S_{q_1 q_2}$ decay nonmonotonically as $\sim(q_1 - q_2\nu)^{-1}$. For a better quantitative understanding, Fig. 5 shows the direct mapping $S_{q_1 q_2}$ versus $k_{z q_1 q_2}$ for the same array configurations as in Fig. 4 and $|q_1|, |q_2| \leq 50$. Apart from the trivial periodic case [Fig. 5(a)], one observes highly-populated spectra, which display perfect periodicity in the case of commensurate scales [Fig. 5(b)] and only some loose repetitiveness otherwise [Fig. 5(c)]. In both cases, a vast majority of the spatial frequencies have amplitude coefficients significantly smaller ($\lesssim -20$ dB) than the dominant ones.

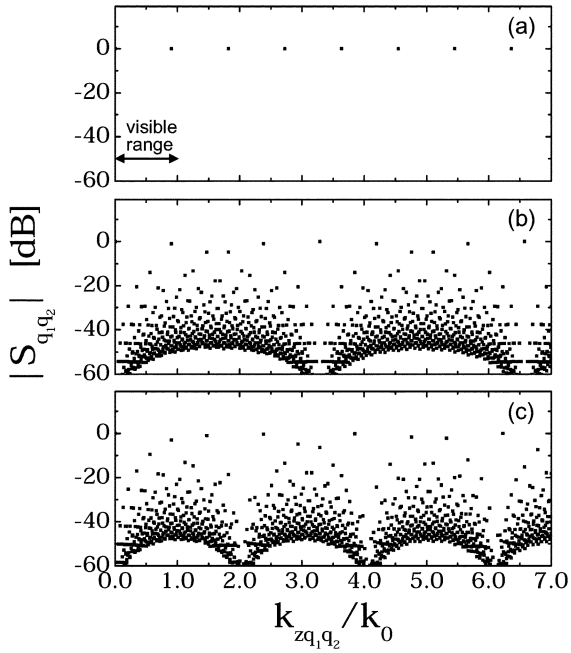

Fig. 5. As in Fig. 4, but $|S_{q_1 q_2}|$ versus $k_{z q_1 q_2}$, for $|q_1|, |q_2| \leq 50$ and $k_{z q_1 q_2} \leq 7k_0$. Due to symmetry, only positive spatial frequencies are shown.

B. Truncation Effects: Semi-Infinite Arrays

Capitalizing on some analogies with the problem expounded in [30], we have also studied truncation-induced diffraction effects. For the semi-infinite $(m \geq 0)$ version of the array in (1), one obtains a *truncated* QF wave synthesis

$$\begin{aligned} A(\mathbf{r}) &= \sum_{m=0}^{\infty} A_m(\mathbf{r}) \\ &= \sum_{m=0}^{\infty} \frac{\exp(-jk_0 R_m)}{4\pi R_m} \exp(-jk_0 \eta z_m) \\ &= \frac{A_0(\mathbf{r})}{2} + \sum_{q_1, q_2 = -\infty}^{\infty} S_{q_1 q_2} A^T_{q_1 q_2}(\mathbf{r}) \end{aligned} \tag{23}$$

where $A^T_{q_1 q_2}$ are *truncated* QF wave propagators

$$\begin{aligned} A^T_{q_1 q_2}(\mathbf{r}) &= \frac{1}{d_{av}} \int_0^{\infty} \frac{\exp(-jk_0 R)}{4\pi R} \exp(-jk_{z q_1 q_2} z')\, dz' \\ &= \frac{\exp(-jk_{z q_1 q_2} z)}{8\pi d_{av}} \int_{-\infty}^{\infty} \frac{\mathrm{H}_0^{(2)}(k_{\rho q_1 q_2} \rho)}{k_z - k_{z q_1 q_2}} dk_z. \end{aligned} \tag{24}$$

Exploiting the uniform high-frequency asymptotic approximation given in [30, eqs. (28)–(35)] for the spectral integral in (24), one obtains

$$A^T_{q_1 q_2}(\mathbf{r}) \sim A^{\mathrm{QF}}_{q_1 q_2}(\mathbf{r}) U\left(\beta^{\mathrm{SB}}_{q_1 q_2} - \beta_d\right) + A^d_{q_1 q_2}(\mathbf{r}). \tag{25}$$

In (25), $A^{\mathrm{QF}}_{q_1 q_2}$ is the QF wave propagator in (20), U denotes the Heaviside unit-step function, $\beta^{\mathrm{SB}}_{q_1 q_2}$ delimits the shadow-boundary of each QF wave (for *propagating* QF waves, $\beta^{\mathrm{SB}}_{q_1 q_2} = \beta_{q_1 q_2}$). Moreover, $A^d_{q_1 q_2}$ represents the *diffracted* QF wave emanating from the array tip

$$A^d_{q_1 q_2}(\mathbf{r}) \sim \frac{\exp(-jk_0 R_d)}{j4\pi d_{av} k_0 R_d} \frac{F(\gamma^2_{q_1 q_2})}{(\cos\beta_{q_1 q_2} - \cos\beta_d)} \tag{26}$$

where $R_d = \sqrt{\rho^2+z^2}$, $\beta_d = \arctan(\rho/z)$, $\gamma_{q_1q_2} = \sqrt{2k_0R_d}\sin[(\beta_{q_1q_2}-\beta_d)/2]$, and F denotes the standard transition function of the uniform theory of diffraction (UTD)

$$F(x) = 2j\sqrt{x}\exp(jx)\int_{\sqrt{x}}^{\infty}\exp\left(-j\xi^2\right)d\xi$$
$$-\frac{3}{2}\pi < \arg(x) \le \frac{\pi}{2}. \tag{27}$$

The wave phenomenologies are illustrated in Fig. 3, for the case of *propagating* ($|k_{zq_1q_2}| < k_0$) QF waves. The region of validity of each QF wave $A^{\mathrm{QF}}_{q_1q_2}$ (heavy arrow in Fig. 3) arriving from direction $\beta_{q_1q_2}$ is now limited by a conical shadow boundary. The spherical tip-diffracted QF wave $A^{d}_{q_1q_2}$ (dashed arrow in Fig. 3) arriving from direction β_d ensures, via the transition function in (27), continuity of the wavefield across the parabolic transition region (gray shading in Fig. 3) surrounding the shadow boundary cone.

Note that *evanescent* ($|k_{zq_1q_2}| > k_0$) QF waves yield negligible contributions at observation points far from the array axis, but they excite *propagating diffracted* fields that need to be taken into account. As in [30] [see the discussion after (35)], these contributions are approximated via *nonuniform* asymptotics [$F \approx 1$ in (26)]. We point out that, at variance with the periodic array case [30, Eq. (36)], it is not possible here to recast the total spherical wave diffracted field in a more manageable form.

V. Results and Potential Applications

Although our main interest in this preliminary investigation is focused on wave-dynamical phenomenologies associated with radiation from quasi-periodic antenna arrays, we briefly discuss some computational and applicational aspects with the hope of providing further insights. We stress that no attempt has been made at this stage to devise *optimal* computational schemes, nor do we deal with actual fabrication-oriented issues (feeding, matching, interelement coupling, etc.).

A. Numerical Results

From a computational viewpoint, the actual utility of the QF syntheses in Section IV (*double* summations involving an *infinite* number of propagating waves) might appear questionable as compared with brute-force element-by-element synthesis. However, as observed in Section IV-A (see also Fig. 5), under appropriate conditions, a large number of propagating QF waves could be *weakly* excited, thus suggesting the possibility, yet to be explored, of devising effective truncation schemes. Here, we try to quantify some of these aspects via numerical examples. We begin by considering a 101-element nonphased standard-Fibonacci array [$\eta = 0, \nu = 1/\tau$, $|m| \le 50$ in (1)]. The truncated QF synthesis developed in Section IV-B for a semi-infinite array can readily be exploited here by expressing the finite array interval as the difference between two overlapping semi-infinite intervals. Fig. 6 shows the near-field ($R = 100\lambda_0$) QF synthesis results for $d_{av} = 0.5\lambda_0$, using the crudest possible truncation criterion based on retaining N_p dominant propagating QF waves in (23). Also shown, as a reference solution, is the element-by-element synthesis in (17) (with $|m| \le 50$). It is observed that the QF synthesis with $N_p = 9$ propagating waves

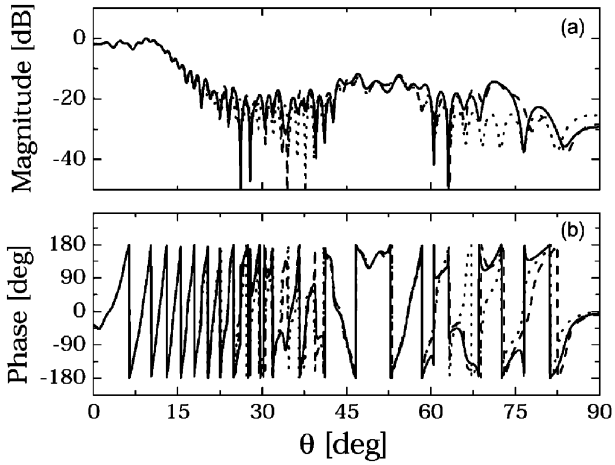

Fig. 6. 101-element standard-Fibonacci ($\nu = 1/\tau$) array with $d_{av} = 0.5\lambda_0$ and $\eta = 0$. Near-zone ($R = 100\lambda_0$) normalized potential field scan.—Reference solution (element-by-element summation); ····· QF synthesis retaining $N_p = 3$ dominant propagating waves (selected within $|q_1|, |q_2| \le 50$); --- QF synthesis retaining $N_p = 9$ dominant propagating QF waves. Due to symmetry, only positive angles are shown.

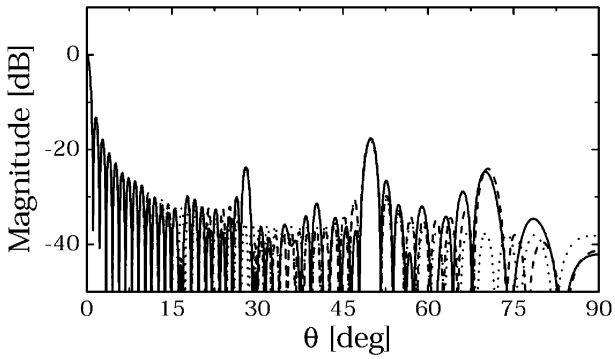

Fig. 7. As in Fig. 6, but far-field pattern.

provides reasonably good agreement, and even $N_p = 3$ is still capable of fleshing out most of the wavefield structure. Similar statements can be made for the far-field pattern in Fig. 7. In order to better quantify the accuracy, and address convergence issues, we have computed the r.m.s. error

$$\Delta A(R) = \sqrt{\frac{\int_{-\pi/2}^{\pi/2}\left|A^{\mathrm{RS}}(R,\theta) - A^{\mathrm{QF}}(R,\theta)\right|^2 d\theta}{\int_{-\pi/2}^{\pi/2}\left|A^{\mathrm{RS}}(R,\theta)\right|^2 d\theta}} \tag{28}$$

where the superscripts "RS" and "QF" denote the reference solution and the QF synthesis, respectively. Fig. 8 shows the error behavior versus the number N_p of dominant propagating QF waves retained, for near-field synthesis (results for the far-field are practically identical). Also shown, for comparison, are results obtained by retaining a number $N_e = N_p$ of dominant evanescent QF diffracted waves. It is observed that a moderate number ($\sim$10) of QF waves is capable of providing acceptable accuracy ($\Delta A \sim -20$ dB). The contribution of N_e retained evanescent QF diffracted waves is practically negligible for $N_e \lesssim 20$, but can give observable improvements at larger N_e-values. Intuitively, one would expect the convergence behavior to improve in the presence of weaker aperiodicity

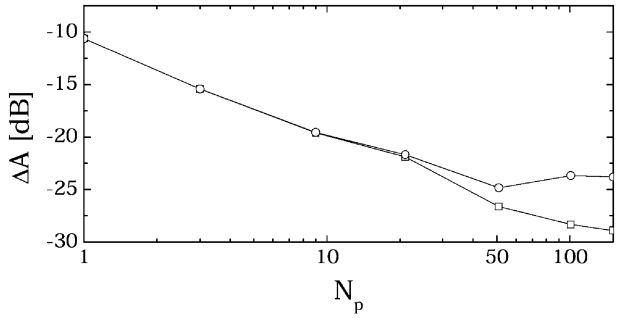

Fig. 8. Parameters as in Fig. 6, but r.m.s. error ΔA in (28) versus number N_p of propagating waves retained in the near field ($R = 100\lambda_0$) QF synthesis. Circular bullets: No evanescent diffracted waves retained. Square bullets: $N_e = N_p$ evanescent diffracted waves retained. Results for the far-field are practically identical.

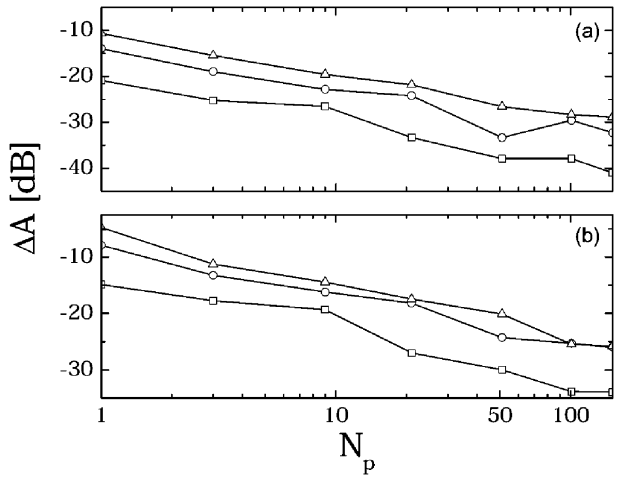

Fig. 9. As in Fig. 8, with $R = 100\lambda_0$, $N_e = N_p$, and various values of scale ratio $\nu = d_2/d_1$ and average spacing d_{av}. (a): $d_{av} = 0.5\lambda_0$. (b): $d_{av} = 0.75\lambda_0$. Square bullets: $\nu = 0.9$. Circular bullets: $\nu = 0.75$. Triangular bullets: $\nu = 1/\tau$.

($\nu \approx 1$) and smaller average interelement spacing, and vice-versa. This is confirmed by the results shown in Fig. 9, for two values of the interelement spacing ($d_{av} = 0.5\lambda_0$ and $0.75\lambda_0$) and three values of the scale ratio ($\nu = 0.9, 0.75$ and $1/\tau$).

To sum up, the above results seem to indicate that moderate-size QF syntheses, truncated by using even crude criteria, can still be capable of capturing the dominant features of the relevant wave dynamics. However, besides the computational convenience, which can become questionable if highly accurate results are needed, the QF parameterization can offer valuable insights for judicious exploitation of the inherent degree of freedom (scale ratio $\nu = d_2/d_1$) in the array (see, e.g., Section V-B).

B. Potential Applications

In view the *discrete* character of its spectrum [see (10b)], the modified-Fibonacci array in (1) does not offer particular advantages within the framework of array thinning, as compared with periodic arrays. In this connection, other 1-D aperiodic sequences, such as the Rudin–Shapiro [20] (characterized by *continuous* spectra), might be worth being explored.

However, the degree of freedom available in the choice of the scale ratio $\nu = d_2/d_1$ can be exploited in principle to control the spectral properties and achieve, for instance, a *multibeam* radiation pattern. As a simple example, we consider a nonphased ($\eta = 0$) configuration with average interelement spacing $d_{av} < \lambda_0$. It is readily observed from (11) and (12) that, besides the unit-amplitude QF wave ($q_1 = q_2 = 0$) (main beam at broadside), the only other propagating QF waves (secondary beams) are

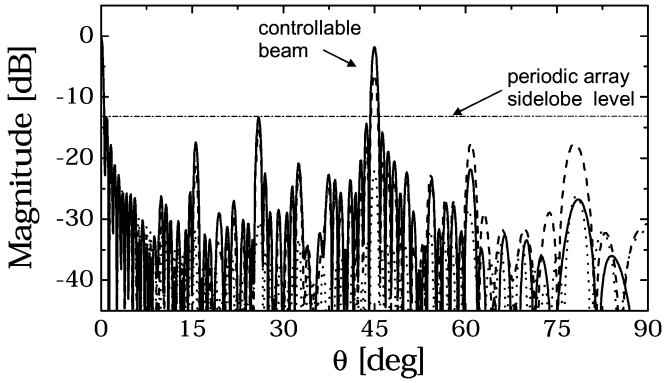

Fig. 10. 101-element modified-Fibonacci array with $d_{av} = 0.874\lambda_0$ and $\eta = 0$. Radiation pattern (array factor) $|\tilde{F}(k_0 \sin\theta)|$ in (10a) (with $|m| \leq 50$) for various values of scale ratio ν, illustrating the controllable multibeam capability (see Section V-B).—$\nu = 0.25$ ($S_{01} = -1.83$ dB); – – – $\nu = 0.5$ ($S_{01} = -6.37$ dB); $\cdots\cdots$ $\nu = 0.9$ ($S_{01} = -23.3$ dB). Note that minor sidelobes never exceed the periodic-array sidelobe level (-13 dB).

$$q_1 = -q_2 = \pm 1, \quad |W_{q_1 q_2}| = \frac{\pi(1+\tau)(1+\nu)}{\nu+\tau} > \pi \tag{29a}$$

$$q_1 = \pm 1, q_2 = 0, \quad |W_{q_1 q_2}| = \frac{\pi(1+\tau)}{\nu+\tau} \geq \pi \tag{29b}$$

$$q_1 = 0, q_2 = \pm 1, \quad |W_{q_1 q_2}| = \frac{\pi\nu(1+\tau)}{\nu+\tau} \leq \pi. \tag{29c}$$

Note that, since $|W_{q_1 q_2}| \geq \pi$, the amplitude of the secondary beams in (29a) and (29b) will *always* be at least 13dB below the main beam, and thus at the same level of sidelobes as in finite-size periodic arrays, *irrespective* of the scale ratio ν. Conversely, for the secondary beam in (29), one has $|W_{q_1 q_2}| \leq \pi$, and thus its amplitude can be controlled over a wide range by varying the scale ratio ν. Restricting attention to the ($q_1 = 0, q_2 = 1$) beam, one finds from (11), (12) the corresponding direction β_{01} (from endfire) and amplitude S_{01} to be

$$\beta_{01} = \arccos\left[\frac{\lambda_0\tau}{d_{av}(1+\tau)}\right], \quad S_{01} = \frac{(\nu+\tau)\sin\left[\frac{\pi\nu(1+\tau)}{\nu+\tau}\right]}{\pi\nu(1+\tau)}. \tag{30}$$

The direction β_{01} can thus be steered, by varying d_{av}/λ_0, up to a maximum value $\beta_{01}^{(\max)} = \arccos[\tau/(1+\tau)] \approx 51.83^o$, corresponding to the maximum spacing ($d_{av} = \lambda_0$) allowable to prevent emergence, in the visible range, of higher-order grating lobes. The amplitude S_{01} can be controlled (from 0 to 1, in principle) by varying the scale ratio $\nu = d_2/d_1$ (from 1 to 0). One thus obtains a *multibeam* radiation pattern with the possibility of controlling the secondary beam amplitude. Results for the ($q_1 = 0, q_2 = -1$) beam follow from symmetry considerations. Obvious fabrication-related issues prevent ν from being exceedingly small, but values of $\nu \approx 0.25$ are sufficient to achieve secondary beam amplitudes ~ -2 dB. Fig. 10 shows the radiation pattern (array factor) of a 101-element array, with d_{av}/λ_0 and ν

chosen from (30) so as to create a secondary beam at 45^o with various amplitudes. It is observed that actual amplitude values are very close to the infinite-array predictions in (30), and that minor sidelobes never exceed the periodic-array sidelobe level (-13 dB).

It is hoped that the above observations might open up new perspectives for reconfigurable arrays. Note that *rational* values of ν (commensurate scales) correspond to configurations interpretable as *periodic* arrays with *aperiodically-distributed* lacunas. In these cases, one can think of easily-implementable reconfigurable strategies, based on switching from *single-beam* (periodic array) to *multibeam* (modified-Fibonacci) radiation patterns, via on-off selection of a set of antenna elements, keeping the average interelement spacing $d_{av} < \lambda_0$.

VI. Conclusions and Perspectives

A simple illustrative example of wave interaction with quasi-periodic order has been discussed in connection with the radiation properties of 1-D antenna arrays, utilizing the modified-Fibonacci sequence. A "quasi-Floquet" analytic parameterization, based on a generalized Poisson summation formula, has been derived for infinite and semi-infinite arrays. Computational issues and potential applications have been briefly addressed.

It is hoped that the prototype study in this paper, through its instructive insights into some of the basic mechanisms governing wave interactions with quasi-periodic order, may lead to new applications in array radiation pattern control, in view of the additional degrees of freedom available in aperiodic structures. Accordingly, we are planning current and future investigations of modified-Fibonacci arrays that will emphasize the effects of the scale ratio parameter ($\nu = d_2/d_1$) on the input impedance as well as on the coupling to possible dielectric-substrate-induced leaky modes. Exploration of the radiation properties of antenna arrays based on other well-understood aperiodic sequences (e.g., Thue–Morse, period-doubling, Rudin–Shapiro [20]) is also being pursued.

Appendix
Pertaining to (10)–(13)

In [27], the modified-Fibonacci array spectrum in (10) is computed using two equivalent approaches, one directly based on the cut-and-project scheme described in Section II-B (see also Fig. 2), and the other based on an "average unit cell" method [32]. Although the two approaches are relatively simple in principle, their implementation is rather involved and not reported here for brevity. The reader is referred to [27], [32] for theoretical foundations and technical details, and to [40], [41] for an alternative approach applicable to rather general substitutional sequences. We point out that in [27], the result for the radiation spectrum is given in normalized form, with a nonexplicit multiplicative constant, and assuming zero phasing ($\eta = 0$). In the paper here, the possible presence of phasing is accounted for via the spectral shift $k_0\eta$ in (12). The calculation of the proper multiplicative constant in (10) (and hence that in (13)) has been accomplished by first observing that for the modified-Fibonacci sequence in (5), the number of array elements falling within a window of width 2ζ approaches the ratio between the window width and the average interelement spacing d_{av} in (7), as $\zeta \to \infty$, i.e.

$$\sum_{m=-\infty}^{\infty} \left[U\left(z_m + \zeta\right) - U\left(z_m - \zeta\right)\right] \sim \frac{2\zeta}{d_{av}} \tag{31}$$

with U denoting the Heaviside step-function. It then follows from (1), assuming $\eta = 0$ and recalling (31), that

$$\begin{aligned} &\lim_{\zeta\to\infty} \frac{1}{2\zeta} \int_{-\zeta}^{\zeta} f(z)dz \\ &\quad = \lim_{\zeta\to\infty} \frac{1}{2\zeta} \sum_{m=-\infty}^{\infty} \left[U\left(z_m + \zeta\right) - U\left(z_m - \zeta\right)\right] \\ &\quad = \lim_{\zeta\to\infty} \frac{1}{2\zeta} \left(\frac{2\zeta}{d_{av}}\right) = \frac{1}{d_{av}}. \end{aligned} \tag{32}$$

The proper multiplicative constants in (10) and (13) have accordingly been computed by requiring that (13) satisfy (32) for $\eta = 0$.

References

[1] D. Shechtman, I. Blech, D. Gratias, and J. W. Cahn, "Metallic phase with long-range orientational order and no translation symmetry," *Phys. Rev. Lett.*, vol. 53, no. 20, pp. 1951–1953, Nov. 1984.

[2] D. Levine and P. J. Steinhardt, "Quasicrystals: A new class of ordered structures," *Phys. Rev. Lett.*, vol. 53, no. 26, pp. 2477–2480, Dec. 1984.

[3] R. J. Mailloux, *Phased Array Antenna Handbook*. Boston, MA: Artech House, 1994.

[4] B. D. Steinberg, "Comparison between the peak sidelobe of the random array and algorithmically designed aperiodic arrays," *IEEE Trans. Antennas Propagat.*, vol. 21, pp. 366–370, May 1973.

[5] Y. Kim and D. L. Jaggard, "The fractal random array," *Proc. of the IEEE*, vol. 74, no. 9, pp. 1278–1280, Sep. 1986.

[6] V. V. S. Prakash and R. Mittra, "An efficient technique for analyzing multiple frequency-selective-surface screens with dissimilar periods," *Microwave Opt. Technol. Letts.*, vol. 35, no. 1, pp. 23–27, Oct. 2002.

[7] C. C. Chiau, X. Chen, and C. Parini, "Multiperiod EBG structure for wide stopband circuits," *IEE Proc. Microwaves, Antennas and Propagat.*, vol. 150, no. 6, pp. 489–492, Dec. 2003.

[8] V. Pierro, V. Galdi, G. Castaldi, I. M. Pinto, and L. B. Felsen, "Radiation properties of planar antenna arrays based on certain categories of aperiodic tilings," *IEEE Trans. Antennas Propagat.*, vol. 53, no. 2, pp. 635–644, Feb. 2005.

[9] B. Grünbaum and G. C. Shepard, *Tilings and Patterns*. New York, NY: Freeman, 1987.

[10] M. Senechal, *Quasicrystals and Geometry*. Cambridge, UK: Cambridge University Press, 1995.

[11] S. Vajda, *Fibonacci and Lucas Numbers, and The Golden Section: Theory and Applications*. New York, NY: Halsted Press, 1989.

[12] R. Merlin, K. Bajema, R. Clarke, F.-Y. Juang, and P. K. Bhattacharya, "Quasiperiodic GaAs-AlAs heterostructures," *Phys. Rev. Lett.*, vol. 55, no. 17, pp. 1768–1770, Oct. 1985.

[13] R. Lifshitz, "Quasicrystals: A matter of definition," *Found. of Physics*, vol. 33, no. 12, pp. 1703–1711, Dec. 2003.

[14] M. Kohmoto, B. Sutherland, and K. Iguchi, "Localization of optics: Quasiperiodic media," *Phys. Rev. Lett.*, vol. 58, no. 23, pp. 2436–2438, Jun. 1987.

[15] D. Würtz, T. Schneider, and M. P. Soerensen, "Electromagnetic wave propagation in quasiperiodically stratified media," *Physica A*, vol. 148, no. 1–2, pp. 343–355, Feb. 1988.

[16] A. Süto, "Singular continuous spectrum on a cantor set of zero Lebesgue measure for the Fibonacci hamiltonian," *J. Stat. Phys.*, vol. 56, pp. 525–531, 1989.

[17] E. Diez, F. Domínguez-Adame, E. Maciá, and A. Sánchez, "Dynamical phenomena in Fibonacci semiconductor superlattices," *Phys. Rev. B*, vol. 54, no. 23, pp. 16 792–16 798, Dec. 1996.
[18] M. S. Vasconcelos, E. L. Albuquerque, and A. M. Mariz, "Optical localization in quasiperiodic multilayers," *J. Phys.: Condens. Matter*, vol. 10, no. 26, pp. 5839–5849, Jul. 1998.
[19] E. Maciá, "Optical engineering with Fibonacci dielectric multilayers," *Appl. Phys. Lett.*, vol. 73, no. 23, pp. 3330–3332, Dec. 1998.
[20] M. S. Vasconcelos and E. L. Albuquerque, "Transmission fingerprints in quasiperiodic multilayers," *Phys. Rev. B*, vol. 59, no. 17, pp. 11 128–11 131, May 1999.
[21] Z. Ouyang, C. Jin, D. Zhang, B. Cheng, X. Meng, G. Yang, and J. Li, "Photonic bandgaps in two-dimensional short-range periodic structures," *J. Opt. A: Pure Appl. Opt.*, vol. 4, no. 1, pp. 23–28, Jan. 2002.
[22] E. Cojocaru, "Omnidirectional reflection from finite periodic and Fibonacci quasiperiodic multilayers of alternating isotropic and birefringent thin films," *Appl. Opt.*, vol. 41, no. 4, pp. 747–755, Feb. 2002.
[23] L. Dal Negro, C. J. Oton, Z. Gaburro, L. Pavesi, P. Johnson, A. Lagendijk, R. Righini, M. Colocci, and D. S. Wiersma, "Light transport through the band-edge states of Fibonacci quasicrystals," *Phys. Rev. Lett.*, vol. 90, pp. 055 501–055 501, Feb. 2003.
[24] J. Baumberg, "When photonic crystals meet Fibonacci," *Phys. World*, vol. 16, no. 4, pp. 24–24, Apr. 2003.
[25] J.-W. Dong, P. Han, and H.-Z. Wang, "Broad omnidirectional reflection band forming using the combination of Fibonacci quasiperiodic and periodic one-dimensional photonic crystals," *Chin. Phys. Lett.*, vol. 20, no. 11, pp. 1963–1965, Nov. 2003.
[26] R. Ilan, E. Liberty, S. E.-D. Mandel, and R. Lifshitz, "Electrons and phonons on the square Fibonacci tiling," *Ferroelectrics*, vol. 305, pp. 15–19, 2004.
[27] P. Buczek, L. Sadun, and J. Wolny, "Periodic diffraction patterns for 1D quasicrystals," *Acta Physica Polonica*, vol. 36, no. 3, pp. 919–933, Mar. 2005.
[28] H. Wei, C. Zhang, Y.-Y. Zhu, S.-N. Zhu, and N.-B. Ming, "Analytical expression for the fourier spectrum of a quasiperiodic Fibonacci superlattice with k components ($k \leq 3$)," *Phys. Stat. Sol. (b)*, vol. 229, no. 3, pp. 1275–1282, Feb. 2002.
[29] L. B. Felsen and F. Capolino, "Time-domain Green's function for an infinite sequentially excited periodic line array of dipoles," *IEEE Trans. Antennas Propagat.*, vol. 48, pp. 921–931, Jun. 2000.
[30] F. Capolino and L. B. Felsen, "Frequency- and time-domain Green's function for a phased semi-infinite periodic line array of dipoles," *IEEE Trans. Antennas Propagat.*, vol. 50, pp. 31–41, Jan. 2002.
[31] M. Severin, "An analytical treatment of diffraction in quasiperiodic superlattices," *J. Phys.: Condens. Matter*, vol. 1, no. 38, pp. 6771–6776, Sep. 1989.
[32] J. Wolny, "Average unit cell approach to diffraction analysis of some aperiodic structures—Decorated Fibonacci chain," *Czech. J. Phys.*, vol. 51, no. 4, pp. 409–419, Apr. 2001.
[33] H. Bohr, *Almost Periodic Functions*. New York, NY: Chelsea, 1947.
[34] A. S. Besicovitch, *Almost Periodic Functions*. New York, NY: Dover, 1954.
[35] A. Papoulis, *The Fourier Integral and Its Applications*. New York, NY: McGraw-Hill, 1962.
[36] L. Carin and L. B. Felsen, "Time-harmonic and transient scattering by finite periodic flat strip arrays: Hybrid (ray)-(floquet mode)-(MOM) algorithm and its GTD interpretation," *IEEE Trans. Antennas Propagat.*, vol. 41, pp. 412–421, Apr. 1993.
[37] L. B. Felsen and L. Carin, "Diffraction theory and of frequency- and time-domain scattering by weakly aperiodic truncated thin-wire gratings," *J. Opt. Soc. Am. A*, vol. 11, no. 4, pp. 1291–1306, Apr. 1994.
[38] L. B. Felsen and E. Gago-Ribas, "Ray theory for scattering by two-dimensional quasi-periodic plane finite arrays," *IEEE Trans. Antennas Propagat.*, vol. 44, pp. 375–382, Mar. 1996.
[39] A. Cucini, M. Albani, and S. Maci, "Truncated floquet wave full-wave analysis of large phased arrays of open-ended waveguides with a nonuniform amplitude excitation," *IEEE Trans. Antennas Propagat.*, vol. 51, pp. 1386–1394, Jun. 2003.
[40] M. Kolář, "New class of one-dimensional quasicrystals," *Phys. Rev. B*, vol. 47, no. 9, pp. 5489–5492, Mar. 1993.
[41] M. Kolář, B. Iochum, and L. Raymond, "Structure factor of 1D systems (superlattices) based on two-letter substitution rules: I. δ (Bragg) peaks," *J. Phys. A: Math. Gen.*, vol. 26, no. 24, pp. 7343–7366, Dec. 1993.

Vincenzo Galdi (M'98–SM'04) was born in Salerno, Italy, on July 28, 1970. He received the Laurea degree (*summa cum laude*) in electrical engineering and the Ph.D. degree in applied electromagnetics from the University of Salerno, Italy, in 1995 and 1999, respectively.

From April to December 1997, he held a visiting position in the Radio Frequency Division of the European Space Research & Technology Centre (ESTEC-ESA), Noordwijk, The Netherlands. From September 1999 to August 2002, he held a Research Associate position in the Department of Electrical and Computer Engineering at Boston University, Boston, MA. In November 2002, he was appointed Associate Professor of Electromagnetics, and joined the Department of Engineering at the University of Sannio, Benevento, Italy, where he is currently working. His research interests include analytical and numerical techniques for wave propagation in complex environments, electromagnetic chaos, and inverse scattering.

Dr. Galdi is a Member of Sigma Xi. He is the recipient of a 2001 International Union of Radio Science (URSI) "Young Scientist Award."

Giuseppe Castaldi was born in Benevento, Italy, in 1968. He received the Laurea degree (*summa cum laude*) in electrical engineering from the "Federico II" University of Naples, Italy, in 1995, and the Ph.D. degree in applied electromagnetics from the University of Salerno, Italy, in 1999.

In 2001, he was a Postdoctoral Research Fellow at the TNO Physics and Electronics Laboratory, The Hague, The Netherlands. In 2003, he was appointed Assistant Professor of Electromagnetics and joined the Department of Engineering at the University of Sannio, Benevento, where he is currently working. His research interests include electromagnetic chaos, quasi-periodic antenna arrays, applications of neural networks to inverse scattering problems, and field representations in complex environments.

Vincenzo Pierro was born in Salerno, Italy, in 1967. He received the Laurea degree (*summa cum laude*) in physics from the University of Salerno, Italy, in 1990.

In 1991, he held a visiting position in the COLUMBUS Metrology Group at the European Space Research & Technology Centre (ESTEC-ESA), Noordwijk, The Netherlands. Since 1996, he has been with the Faculty of Engineering, University of Sannio, Benevento, Italy, where he was appointed Assistant Professor of Electromagnetics in 1996, and Associate Professor in 2001. His main research interests are in the field of complex electromagnetic systems, electromagnetic detection of gravitational waves, and applied mathematics.

Dr. Pierro is a Member of the Italian Physical Society (SIF). He was awarded a research fellowship in 1999 from the Japan Society for the Promotion of Science (JSPS), in connection with the TAMA 300 experiment.

Innocenzo M. Pinto (M'99) was born and educated in Italy.

Winner of national competitions, he was appointed Assistant Professor of Electromagnetics in 1983, Associate Professor in 1987, and Full Professor in 1990. He has been a faculty member in the Universities of Naples, Salerno (where he founded and chaired the Ph.D. program in Information Engineering from 1993 to 2001), Catania, and Sannio at Benevento, where he is currently the Dean of the Information Engineering Curricula Committee. He has visited several research institutions as an invited lecturer, including CERN, KEK, and NIST (former NBS). In 1998, he was an EU Senior Visiting Scientist at the National Astronomical Observatory, Tokyo, Japan, in connection with TAMA300 experiment. He authored or co-authored more than 100 technical papers in peer-reviewed international journals. His research interests span from electrophysics to gravitational wave experiments.

Dr. Pinto is a Member of the American Physical Society.

Leopold B. Felsen (S'47–M'54–SM'55–F'62–LF'90) was born in Munich, Germany, on May 7, 1924. He received the B.E.E., M.E.E, and D.E.E. degrees from the Polytechnic Institute of Brooklyn, Brooklyn, NY, in 1948, 1950, and 1952, respectively.

He emigrated to the United States in 1939 and served in the U.S. Army from 1943 to 1946. After 1952 he remained with the Polytechnic (now Polytechnic University), becoming University Professor in 1978. From 1974 to 1978 he was Dean of Engineering. In 1994 he resigned from the full-time Polytechnic faculty and was granted the status of University Professor Emeritus. He is now Professor of aerospace and mechanical engineering and Professor of electrical and computer engineering at Boston University, Boston, MA (part-time). He is the author or coauthor of more than 350 papers and of several books, including *Radiation and Scattering of Waves* (Piscataway, NJ: IEEE Press, 1994). He is an Associate Editor of several professional journals and was an Editor of the Wave Phenomena Series (New York: Springer-Verlag). His research interests encompass wave propagation and diffraction in complex environments and in various disciplines, high-frequency asymptotic and short-pulse techniques, and phase-space methods with an emphasis on wave-oriented data processing and imaging.

Dr. Felsen is a Member of Sigma Xi and a Fellow of the Optical Society of America and the Acoustical Society of America. He has held named Visiting Professorships and Fellowships at universities in the United States and abroad, including the Guggenheim in 1973 and the Humboldt Foundation Senior Scientist Award in 1981. In 1974 he was an IEEE Antennas and Propagation Society (APS) Distinguished Lecturer. His "Poet's Corner" appears sporadically in the IEEE/APS Magazine. He received the IEEE/APS Best Paper Award for 1969 and was best paper co-author for 1974 and 1981. He was a contributing author to papers selected for the R. W. P. King Award for 1984, 1986, and 2000. He received the Balthasar van der Pol Gold Medal from the International Union of Radio Science (URSI) in 1975, an Honorary Doctorate from the Technical University of Denmark in 1979, the IEEE Heinrich Hertz Gold Medal for 1991, the APS Distinguished Achievement Award for 1998, the IEEE Third Millennium Medal in 2000, an honorary Laurea degree from the University of Sannio in Benevento, Italy in 2003, the IEEE Electromagnetics Award for 2003, an honorary doctorate from the Technical University of Munich, Germany in 2004, three Distinguished Faculty Alumnus Awards from Polytechnic University, and an IEEE Centennial Medal in 1984. In 1977, he was elected to the National Academy of Engineering. He served on the APS Administrative Committee from 1963 to 1966 and was Vice Chairman and Chairman for both the US (1966–1973) and the International (1978–1984) URSI Commission B.